Markerless tracking suggests a tactile sensing role for spider forelegs during locomotion

Running title: Markerless tracking of spider locomotion

Kiri F. Pullar and Michael G. Paulin

Department of Zoology, University of Otago, P O Box 56, Dunedin, New Zealand

Corresponding author's email address: kiri.pullar@otago.ac.nz

Keywords: arthropod, locomotion, gait, kinematic, motion capture, machine vision.

12   **Summary statement:**

13   We developed a machine vision technique for markerless tracking of locomotion in the spider

14   *Dolomedes aquaticus.* Gait analysis suggests that each pair of legs plays a specific role in

15   locomotion.

16   **Abstract**

17   Because of their rigid exoskeleton with relatively simple joint mechanics, arthropods can

18   provide useful models for studying the sensory-neural and mechanical design principles of

19   agile animal locomotion. Gait analysis usually requires attaching markers or manually

20   identifying reference points in video frames, which can be time consuming and inaccurate,

21   especially with small animals. Here we describe a markerless motion capture technique and its

22   application to gait analysis in the New Zealand semi-aquatic hunting spider, *Dolomedes*

23   *aquaticus*. Our machine vision approach uses a model of the spider's skeleton to automatically

24   infer the location of the centre of mass and the configuration of the skeleton in video frames.

25   We found that stride length and frequency are correlated with running speed. Inter-limb

26   coordination during the gait cycle suggests that different legs have specialized roles in

27   locomotion. Phase relationships among the six hindmost legs exhibit an alternating tripod gait,

28   like a hexapod insect. The middle two leg pairs appear to be primarily responsible for

29   generating thrust, while the hind legs contribute more to stability. The front legs are not phase-

30   coupled to the other legs and appear to be used as tactile probes during locomotion. Our

31   machine vision approach has the potential to make arthropod gait analysis faster and simpler.

32   Our results indicate how specialization of limb function may contribute to locomotor efficiency

33   and agility of a specialized hunting spider, and how arthropod design principles may contribute

34   to developing efficient, agile legged robots.

35

Introduction

Arthropods have proven favourable subjects for studies of locomotion for over a century (Bowerman, 1977). Apart from being of interest in their own right, there are several reasons why investigations into the neural, morphological and mechanical mechanisms underlying arthropod locomotion have broader appeal. Firstly, locomotion is essential for life in the majority of organisms, playing an important role in interactions between mates, predators and prey. Secondly, repeated stereotyped behaviour can be produced with relative ease which allows for descriptive, quantitative and neurophysiological analyses (Bowerman, 1977). Finally, the characteristic rigid exoskeleton and jointed limbs of arthropods can be represented as a rigid body linkage, in which most joints only have a single degree of freedom. Despite major morphological and physiological differences fundamental patterns appear to exist in locomotion, thus generalizations in arthropods can be extrapolated to make predictions in systems of greater complexity e.g. vertebrates and robots (Dickinson et al., 2000).

Although arachnids are one of the largest arthropod groups, study of their locomotory behaviour has been somewhat neglected compared to insects and crustaceans. While the collection of studies is smaller in magnitude they still amount to a reasonably comprehensive analysis of various aspects of locomotion: behavioural descriptions of normal locomotion (Biancardi et al., 2011; Bowerman, 1975a; Shamble et al., 2017; Spagna et al., 2011; Ward and Humphreys, 1981; Weihmann, 2013; Wilson, 1967; turning - Land, 1972; water surface - Shultz, 1987; temperature dependence - Booster et al., 2015; prey strikes - Zeng and Crews, 2018), behavioural descriptions of experimentally modified animals (load carrying - Moffett and Doell, 1980; legs removed or immobilized - Amaya et al., 2001; Apontes and Brown, 2005; Bowerman, 1975b; Gerald et al., 2017; Wilson, 1967), joint kinematics (Blickhan and Barth, 1985; Booster et al., 2015), neurophysiological examinations (Bowerman, 1976; Bowerman and Burrows, 1980; Fourtner and Sherman, 1973; Maier et al., 1987), anatomy of locomotor appendages (Blickhan and Barth, 1985; Bowerman and Burrows, 1980; Dillon, 1952; Fourtner and Sherman, 1973; Parry, 1957; Reußenzehn, 2008; Reußenzehn, 2010), biomechanics (Anderson and Prestwich, 1975; Blickhan, 1986; Blickhan and Barth, 1985; Ellis, 1944; Parry and Brown, 1959a; Reußenzehn, 2010; Sensenig and Shultz, 2006; Shultz, 1991; Siebert et al., 2010; Wilson, 1970; Wilson and Bullock, 1973) and dynamics of locomotion (Biancardi et al., 2011; Blickhan and Barth, 1985; Sensenig and Shultz, 2006; Spagna et al., 2007; Spagna et al., 2011; Weihmann, 2013; jumping - Parry and Brown, 1959b; prey strikes - Zeng and Crews, 2018).

69   The present study focuses on the stepping patterns and kinematics involved with normal
70   spider locomotion. Similar analyses mentioned above generally used one of two approaches.
71   Marker-based techniques, which involve the placement of markers (e.g. paint, nail polish, paper
72   or tape) onto the centre of a joint or tip of a limb. The marker is then tracked in video frames,
73   usually through the aid of commercial software packages. Alternatively, the researcher
74   manually digitized points of interest in each frame through the use of a stop-motion projector.
75   Both approaches are laborious in nature and require careful attention, the first at the beginning
76   of the experiment to ensure the correct placement of markers and the second during processing
77   to accurately locate points of interest. These problems are compounded when working with
78   smaller animals, where positioning of markers, sensors or points of interest is more critical in
79   an accurate description of locomotor kinematics (Gambaretto and Corazza, 2009). This limits
80   the researcher's ability to examine locomotion, as markers can interfere with the animals
81   normal movement and behaviour (Bender et al., 2010). Additionally, although maker-based
82   approaches are widely accepted, they come with intrinsic problems e.g. ghost markers,
83   occlusions of markers, markers can move or become completely removed during locomotion
84   and often require specialized lab environments and lighting conditions. To address the concerns
85   above, we developed semi-automated model-based tracking technique that can capture the 2D
86   motion of the body and leg segments from a high-speed video sequence.

87   Advances in imaging and computer vision are enabling increasingly complete records of
88   animal motion (Brown and Bivort, 2018). Robust approaches for tracking and analysis of body
89   movements have been used to examine locomotion in a variety of animals. Dimensionality
90   reduction methods can be used to identify pixels of video frames that change during animal
91   behaviour and match spatio-temporal image features to exemplar postures, behaviours, or gaits
92   (Berman et al., 2014; Favreau et al., 2006; Gibson et al., 2003; Klibaite et al., 2017). Pixel-
93   based representations can be applied to animals regardless of their shape or limb configuration
94   (Brown and Bivort, 2018), however accuracy of tracking is often improved by utilizing
95   information about the shape, appearance, and/or kinematic structure of subject being tracked
96   (Moeslund et al., 2006).

97   Model-based approaches incorporate information about the subject to estimate its most
98   likely pose given the image sequences (Brown and Bivort, 2018). A motion model was
99   developed to track wallaby locomotion, estimating the pose of a kinematic chain from frame
100   to frame (Bregler et al., 2004). The study originally intended to examine locomotion via a
101   marker-based approach, however it became clear that the locations of makers could not be
102   accurately tracked due to soft tissue deformations (Bregler et al., 2004). Models can be

103 extended to deform not only a skeleton (i.e. the kinematic chain), but also the non-rigid

104 deformation of the 3D surface (i.e. clothing, skin or fur). Several studies of dog locomotion

105 have used probabilistic approaches to match a body shape model to the corresponding

106 silhouette in image frames (Gall et al., 2009; Gambaretto and Corazza, 2009). Few studies have

107 implemented similarly robust methods with the precision required for automated, markerless,

108 tracking of arthropod bodies and appendages (Uhlmann et al., 2017).

109 An investigation of flight kinematics in *Drosophila*, used an accurate geometric fly model,

110 scaled motion dynamics and image registration to capture body and wing rotations (Fontaine

111 et al., 2009). While the kinematic chain in this case required relatively few degrees of freedom,

112 its ability to track a very small animal during complex behaviours is impressive. Recently, a

113 markerless approach has also been applied to leg segment tracking in freely walking

114 *Drosophila* (Uhlmann et al., 2017). FlyLimbTracker used a body and leg model defined by

115 active contours, for a semi-automatic approach which drastically reduced the user intervention

116 required in tracking compared to manual digitization (Uhlmann et al., 2017). In addition to

117 providing important information regarding locomotor parameters, high resolution recording

118 and analyses also can assess the role of proprioceptive sensory inputs during coordinated leg

119 movements (Gowda et al., 2018).

120 In the present study we develop a semi-automated, model-based, markerless approach for

121 tracking freely moving spiders. We focused on providing a detailed analysis of locomotory

122 kinematics without the need for a sophisticated lab setup, expensive commercial software or

123 manual digitization of joint location in each frame. Based on the 2D position of joints in each

124 frame we extract data on the trajectory and coordination of each of the four pairs of legs and

125 compare the results to existing literature.

126 **Materials and methods**

127 *Animals*

128 The experimental procedure consisted of filming the locomotor patterns of unrestrained

129 *Dolomedes aquaticus* Goyen. This species is commonly found near water on or under

130 surrounding objects such as plants, stones and pieces of wood. *D. aquaticus* sense insects and

131 small vertebrates both on water and land by detecting vibrations using the two front pairs of

132 legs (Forster and Forster, 1999). They then chase down their prey with rapid bursts of speed.

133 Only relatively large, adult, female spiders possessing all eight legs were used during filming

134 (mass = 1.194 g $\pm$ 0.376; mean $\pm$ S.D.).

135

Experimental approach

Behavioural arenas consisted of a custom made 40 cm × 10 cm × 2 cm glass arenas; this size was selected as large enough for free locomotion but small enough to encourage spiders to run in a relatively straight line. The arena was lit from below using three 10 × 10 arrays of ultra-bright LEDs. In order to achieve a more uniform light intensity, layers of frosted glass and frosted paper were used to scatter the light from the LEDs. A piece of cardboard covered the last 5 cm at one end to the spider to act as a refuge from the bright light. A 1 cm grid was printed onto an overhead projector transparency overlaid on the arena. The video camera was positioned in the middle, above the arena, to allow filming of the spider from a dorsal viewpoint (Fig. 1A). Trials were recorded using a high-speed video camera (125 fps, 1/625 s shutter speed, 1280 × 1024 pixels with a Troubleshooter 1000 HR, Fastec Imaging, San Diego, USA).

Spiders were occasionally stimulated to move from one end of the arena to the other by either prodding them with tweezers or gently blowing on them. The resulting locomotion did not appear to differ from normal running in unstimulated animals. Each animal was run no more than five consecutive times. Short rest periods were given between each trial while data was transferred from the camera to the computer and converted into HD resolution avi files using the camera software (CamLink, Fastec Imaging, San Diego, USA). Trials where the animal did not run in a straight line or at a near constant speed were rejected. The animals were not observed slipping on the glass surface and did not appear to have any difficulty running. Starting and stopping sequences were not used in analysis.

The locomotor patters of 15 spiders were filmed and their kinematic parameters analysed. Of the many sequences filmed, only a small portion were selected for analysis on the basis of the requirements of constant velocity and straight-line locomotion (N=29). The number of sequences is small due to the small portion of trails that were suitable for analysis as well as the lengthy process involved in pose estimation.

Pose estimation algorithm

This section will briefly describe the algorithm used to estimate the pose of the subject in each frame. This is done using the PoseCut algorithm, which involves energy minimization based on a Conditional Random Field (CRF) in order to estimate the pose of the subject in each frame of a video sequence, as well as segment each frame into subject and background (Bray et al., 2006). The pose estimation code was based around adapting the techniques used by Rasmus Jensen for analysis of human gait using a time of flight camera and is available on request. The pose estimation algorithm is briefly described below, for further detail see Jensen et al. (2009).

169   A frame of the sequence (Fig. 2A) can be treated as set of discrete random variables $\boldsymbol{y} = y_1,$

170    $y_2, ..., y_n,$ where each y_i represents the intensity of the pixel i of an image containing n pixels.

171   The solution to our image segmentation problem becomes finding the value of the vector $\boldsymbol{x} =$

172    $x_1, x_2, ..., x_n$ where each x_i represents the label assigning pixel i to an object. Each x_i takes its

173   value from the label set $L = l_1, l_2, ..., l_m,$ which in our case is a binary problem with labels

174   consisting only of 'background' and 'subject'.

175   The first term of the energy function is a likelihood term, which is based on the intensity

176   distribution of background pixels (Fig. 2B). This term is calculated as the negative log

177   likelihood:

178    $$\phi(\boldsymbol{y}|x_i = background) = -\log P(\boldsymbol{y}|x_i = background). \tag{1}$$

179   Assuming the background pixels have distribution with mean, μ_B, and standard deviation, σ_B,

180   the probability that observed data, $\boldsymbol{y}$, belongs to the background is given by:

181    $$P(\boldsymbol{y}|x_i = background) = \frac{1}{\sqrt{2\pi\sigma_B^2}} \exp\left(-\frac{(\boldsymbol{y} - \mu_B)^2}{\sigma_B^2}\right). \tag{2}$$

182   By taking the negative log of the probability function and discarding the normalization

183   constant, this becomes:

184    $$\phi(\boldsymbol{y}|x_i = background) = \frac{(\boldsymbol{y} - \mu_B)^2}{\sigma_B^2}. \tag{3}$$

185   The beginning of each sequence contained at least 5 frames of background before the subject

186   entered the arena. Thus, the intensity distribution is estimated by simply calculating the mean

187   and standard deviation of each pixel in known background frames.

188   The second term of the energy function is the smoothness prior, which specifies

189   neighbouring pixels will have a higher probability of having the same label. The prior takes the

190   form of a generalized Potts model (Bray et al., 2006):

191    $$\psi(x_i, x_j) = \begin{cases} K_{i,j} & x_i \neq x_j \\ 0 & x_i = x_j \end{cases}, \tag{4}$$

192   where $K_{i,j}$ is a term that penalizes adjacent neighbours which have different labels. Because we

193   are dealing with the binary situation of segmenting between background and subject the

194   problem is referred to as an Ising model (Greig et al., 1989).

195   Additionally, it is assumed that neighbouring pixels with the same label will have similar

196   intensity value. A contrast term is incorporated by increasing the cost within the Ising model

197   proportionally to the similarity in intensity of the corresponding pixels. Thus, penalizing

198   neighbours with similar intensity values which have differing labels:

199
$$\phi(\mathbf{y}|x_i, x_j) = \begin{cases} \lambda \exp\left(\dfrac{-g^2(i,j)}{2\sigma_B^2}\right) & x_i \neq x_j \\ 0 & x_i = x_j \end{cases}, \tag{5}$$

200 where the parameter λ controls the magnitude of the penalty and $g^2(i, j)$ is the gradient, which

201 is approximated via convolution of the image with gradient filters in both in horizontal and

202 vertical directions.

203 The final term in the energy formulation is a shape prior, this looks for an object with known

204 shape and plays an important role in pose estimation. An articulated stick spider model is used

205 to generate a pose-specific shape prior on the segmentation. The stick spider is based on

206 measurements of the length and maximum joint angles of each leg segment for *D. aquaticus*

207 (Reußenzehn, 2008). Given an estimate of the location and shape of the subject, the pose-

208 specific prior is constructed so that pixels falling close to the shape have a higher probability

209 of being labelled 'subject' while those falling further away have a higher probability of being

210 labelled 'background'.

211 The cost of the shape prior is defined as:

212
$$\phi(x_i|\theta) = -\log P(x_i|\theta), \tag{6}$$

213 where θ contains the configuration of the stick spider (position, orientation and leg span). The

214 probability $P(x_i|\theta)$ of x being labelled as subject or background is defined as:

215
$$P(x_i = subject|\theta) = 1 - P(x_i = background|\theta) = \frac{1}{1 + exp(\mu \times d(i,\theta) - d_r)}, \tag{7}$$

216 where $d(i,\theta)$ the distance of pixel i from the shape defined by θ, d_r is the thickness of the shape

217 and μ contains the magnitude of the cost for points outside of the shape. To calculate the

218 distance of each pixel from the shape, the rasterized model (Fig. 2C) undergoes the Euclidean

219 distance transform, resulting in a distance map where pixels that are part of the shape get value

220 zero, those adjacent to the shape get value 1 and so on increasing in magnitude (Fig. 2D).

221 The combination of the terms described above is the energy formulation (Fig. 2E) that is

222 used both to segment the frames and estimate the pose of the subject (Fig. 2F):

223
$$E = \sum_{i \in n} \left(\phi(\mathbf{y}|x_i) + \phi(x_i|\theta) + \sum_{j \in N_i} \left(\psi(x_i, x_j) + \phi(\mathbf{y}|x_i, x_j) \right) \right). \tag{8}$$

224 This energy corresponding to the configuration of the CRF is minimized using the graph cuts

225 approach (Boykov and Kolmogorov, 2004). Each frame requires an initial guess which is

226 optimized to find the estimated pose. In this case the algorithm begins with the pose of the

227 subject in the previous frame updated under the assumption of smooth motion. The assumption
228 of constant velocity provides an initial guess.

229   The only frame requiring manual initialization is the first frame used for tracking. A
230 Graphical User Interface (GUI) was created to allow the user to set the starting pose of the
231 spider in a frame of each video clip and save the coordinates for batch processing later. After
232 the video was loaded and cropped to contain the tracking region of interest, the GUI allowed
233 the user to adjust the global position, angles and leg span of the spider. For estimating the
234 angles, it generally suffices to only set the body-coxa joint for each leg and global rotation. The
235 body and segment lengths defined in the shape model are used to create a model of the spider
236 that has been adjusted for leg span but retains the relative proportions of each segment. The
237 shape model is used to extract configuration values for body position and orientation and the
238 joint angles in each frame.

239 *Gait analysis*

240 Prior to analysis, all raw configuration data was smoothed using a fourth-order, zero-lag
241 Butterworth filter with cut-off frequency uniquely determined for each of the x-y and angular
242 positions. Residual analysis was used in each case to determine an appropriate cut-off
243 frequency (Winter, 1990). Velocity and acceleration of the smoothed linear and angular data
244 were approximated using the numerical method of finite differences.

245   The overall angular movement of the leg was approximated by the angle delimited by the
246 tarsus, the body-coxa joint and the body-coxa joint of the contralateral leg (Fig. 1B). Angles
247 are reported with zero being perpendicular to the mid line of the cephalothorax. These angles
248 increased when the leg moved forwards, reaching a maximum corresponding to the anterior
249 extreme position (AEP) and decreased when the leg moved backwards, reaching a minimum
250 corresponding to the posterior extreme position (PEP). The above system is maintained for
251 individual joints with zero being perpendicular to the mid line of the cephalothorax for the
252 body-coxa joint and the remaining angles are reported as rotation about the line from joint to
253 parent (Fig. 1C).

254   The period of the stride was defined as the time elapsing between two successive AEPs of
255 the same leg. It could only be measured to within 8 ms because of the film speed. The period
256 consisted of one stance phase and one swing phase. The stride frequencies were calculated by
257 1/stride duration and presented as the number of strides per second. Stride length was calculated
258 by dividing the average speed by the stride frequency. The kinematic duty factor (stance
259 duration/stride duration) was expressed as percentage of stride duration. Within a given
260 sequence, stride duration measurements did not differ significantly between legs ($p > 0.05$

261 ANOVA); however, the movements of legs 1 and 4 are more ambiguous for functional reasons

262 i.e. dragging being included as part of protraction. Thus, unless stated otherwise, stride data is

263 presented using leg L2 for comparisons.

264 Phase relationships between legs during locomotion were calculated by the time at which

265 an AEP occurred for a given leg relative within the period of the reference leg (Jamon and

266 Clarac, 1995):

$$\phi_{n:n'} = \frac{(AEP_n - AEP_{n'})}{P_{n'}}, \tag{9}$$

267

268 where $P_{n'}$ is the stride period of the reference leg. Values of ϕ less than 0.25 or greater than

269 0.75 represent simultaneous in-phase stepping and values of ϕ between 0.25 and 0.75 represent

270 alternate anti-phase stepping.

271 *Statistical analysis*

272 All graphing and statistical analyses were performed in MATLAB (Student version R2009a,

273 The MathWorks, USA). We used linear regression, one-way ANOVA and Tukey's post hoc

274 tests to analyse corresponding data. Descriptive statistics are presented as mean ± S.D., and the

275 significance level is set at α=0.05. Comparisons relating kinematic parameters to speed were

276 presented for each trial (N=29). Analysis of phase lags required that at least two full strides

277 were completed by each leg, reducing the number of trials (N=27).

278 For phase lag data, each phase value was multiplied by 360 to convert from phase range (0-

279 1) to degrees (0-360). The mean angle (phase) of leg lag was calculated in MATLAB as:

$$\mu_p = \mathrm{atan2}(y, x), \tag{10}$$

280

281 where *atan2* is a variant of the arctangent function, $x = \sum_{i=1}^{n} \cos\left(\frac{a_i}{n}\right)$, $y = \sum_{i=1}^{n} \sin\left(\frac{a_i}{n}\right)$, and

282 n is the sample size (Fisher, 1995). This value is then divided by 360 to convert the result back

283 to the original range. The circular standard deviation was calculated as:

$$s_p = \frac{180}{\pi} \sqrt{-2 \ln r}, \tag{11}$$

284

285 where r is the length of the mean vector, $r = \sqrt{x^2 + y^2}$ (Zar, 1996). Again, this value is then

286 divided by 360 to convert the result back to the original range. Phase distributions were tested

287 for uniformity of distribution using the Rayleigh test. Rayleigh's z:

$$z = \frac{R^2}{n}, \tag{12}$$

288

289 where $R = nr$ (Zar, 1996). The p value associated with Rayleigh's R is approximated by:

$$p = \exp\left[\sqrt{1 + 4n + 4(n^2 - R^2)} - (1 + 2n)\right], \tag{13}$$

290

291   which is accurate to three decimal places for samples sizes as small as ten (Zar, 1996). To

292   determine if any relationship existed between phase lags and speed, data was examined for

293   angular-linear correlation. The correlation coefficient was calculated as:

294
$$r_{al} = \sqrt{\frac{r_{XC}^2 + r_{XS}^2 - 2r_{XC}r_{XS}r_{CS}}{1 - r_{CS}^2}}, \qquad (14)$$

295   where r_{XC} is the correlation between X (speed) and the cosine of a (phase), r_{XS} is the correlation

296   between X and the sine of a and r_{CS} is the correlation between the sine and cosine of a (Zar,

297   1996). The significance of the correlation is assessed by comparing the test statistic nr_{al}^2 to X^2

298   distribution with 2 degrees of freedom (Zar, 1996).

299   **Results**

300   The locomotion speed measured in 15 individuals during a total of 29 sequences averaged

301   24.807 ± 6.698 cm s^{-1} and ranged between 5.000 and 49.548 cm s^{-1}. Stepping pattern diagrams

302   (Fig. 3) for a range of speeds revealed several trends in locomotor parameters which were

303   investigated in more detail. Stride frequency increased linearly with both absolute (y = 3.793

304   + 0.134x, R^2=0.424, $F_{1,27}$=19.848, p<0.001) and normalized speed (y = 3.174 + 0.309x,

305   R^2=0.580, $F_{1,27}$=37.360, p<0.001). Stride length also increased linearly with both absolute (y =

306   1.694 + 0.075x, R^2=0.464, $F_{1,27}$=23.331, p<0.001) and normalized speed (y = 2.171 + 0.108x,

307   R^2=0.249, $F_{1,27}$=8.949, p=0.006). Stride frequency was more highly correlated with normalized

308   speed and stride length was more highly correlated with absolute speed.

309   The positive trend between stride frequency and speed suggests the lengths of the

310   protraction and/or retraction phases may also have a relationship with speed and stride

311   frequency. Both protraction and retraction periods decreased with absolute (protraction: y =

312   0.105 − 0.001x, R^2=0.284, $F_{1,27}$=10.703, p=0.003; retraction: y = 0.121 - 0.002x, R^2=0.323,

313    $F_{1,27}$=13.034, p=0.001) and normalized speed (protraction: y = 0.111 - 0.003x, R^2=0.384,

314    $F_{1,27}$=16.808, p<0.001; retraction: y = 0.128 − 0.004x, R^2=0.426, $F_{1,27}$=20.063, p<0.001).

315   However, there was a much stronger correlation with stride frequency (protraction: y = 0.145

316   - 0.010x, R^2=0.691, $F_{1,27}$=60.262, p<0.001; retraction: y = 0.172 - 0.013x, R^2=0.821,

317    $F_{1,27}$=123.582, p<0.001). The above data shows the duration of protraction is proportional to

318   both speed and stride frequency, but this does little to inform us how the leg is actually moving

319   through space during the swing phase. We now examine variables relating to the position,

320   velocity and acceleration across the duration of the stride.

321

322

Stepping pattern

While stepping pattern diagrams revealed some general trends, there is variation between sequences (Fig. 3). The stepping order for the ipsilateral legs in both Fig. 3B,C is 4 1 3 2. However, at the slowest speed there is no consistent pattern over the sequence (Fig. 3A). The stepping pattern of spiders can be explained by two models of coupling of legs. Considering the coordination of ipsilateral legs, adjacent legs tend to step alternately and adjacent-but-one legs step together. The resulting pattern is a metachronal wave propagating either anteriorly or posteriorly (Fig. 3B). At faster speeds an additional pattern exists, contralateral legs also alternate, resulting in an alternating tetrapod where diagonally adjacent contralateral legs (L1, R2, L3, R4 and R1, L2, R3, L4) step together (Fig. 3C). While movement of the legs is not exactly synchronized, it does appear that appendages can be divided into two functional groups (Fig. 3C(ii)). An alternative representation of leg coordination is a quantitative analysis of relationships between leg pairs, rather than considering several legs at once. This will further illustrate that despite variation between individual steps and trials consistent patterns exist in spider leg coordination.

Phase relationships between legs

By plotting the time of occurrence of an AEP for a given leg, relative to the stride period of a reference leg, the relationship between timing of leg movements can be scrutinized through a phase histogram (Fig. 4). The mean value of the histogram indicates the relative timing of the movement of the given leg with respect to the reference leg, and the variance gives an indication of the strength of coupling between legs.

The phase lag distributions of contralateral legs all have a mean of approximately 0.5, the value expected from an alternating tetrapod gait (Fig. 4A,B). This result is predicted by Hughes' (1952) rule for contralateral coupling during normal walking, which states that "each leg alternates with the contralateral limb of the same segment". In contrast to the idea of alternating sets of legs, the phase relationship in leg pair 1 showed no clear unimodal distribution ($p > 0.05$, Rayleigh test for uniformity). The phase lags of R1:L1 were rather randomly distributed around the trigonometric circumference (Fig. 4A). All leg pairs have mean phase lags close to 0.5, but appear to have stricter coupling towards the posterior end (mean angle ± circular S.D.: Leg pair 1 = 0.458 ± 0.006, leg pair 2 = 0.498 ± 0.003, leg pair 3 = 0.485 ± 0.002, leg pair 4 = 0.510 ± 0.002).

A similar trend is observed from anterior to posterior in adjacent ipsilateral legs (Fig. 4C,D). Phase lag distributions of pairs containing leg 1 have a greater spread than those which do not contain leg 1 (mean angle ± circular S.D.: L1:L2 = 0.368 ± 0.004, R1:R2 = 0.377 ± 0.005,

357 L2:L3 = 0.437 ± 0.002, R2:R3 = 0.461 ± 0.002, L3:L4 = 0.493 ± 0.002, R3:R4 = 0.512 ±

358 0.002). It is clear that the mean phase value also increased from the anterior to the posterior

359 pairs of adjacent ipsilateral legs. A possible mechanism for this pattern is provided by Hughes'

360 (1952) rule for ipsilateral coupling during normal walking, which states that "no fore or middle

361 leg is protracted until the leg behind has taken up its supporting position".

362   The remaining couplings for adjacent-but-one and adjacent-but-two ipsilateral legs have

363 probably come about as a result of the above two rules (Fig. 4E-G). Again, results can be split

364 into groupings based on whether the pairing contains leg 1 or not (mean angle ± circular S.D.:

365 L1:L3 = 0.823 ± 0.005, R1:R3 = 0.654 ± 0.005, L2:L4 = 0.936 ± 0.003, R2:R4 = 0.972 ± 0.003,

366 L1:L4 = 0.207 ± 0.005, R1:R4 = 0.163 ± 0.005).

367   There was no clear unimodal distribution of R1:R3 phase lags ($p > 0.05$, Rayleigh test for

368 uniformity) and the remaining pairs containing either of the front legs have a more varied

369 distribution than pairs which do not contain either of the front legs. Apart from the pairing of

370 R1:R3 the remaining mean angles are all $\mu > 0.75$ or $\mu < 0.25$ indicating that these legs are

371 moving in-phase.

372   The possibility that phase lag might change with speed was investigated by angular-linear

373 correlation. The phase lag between left legs 3 and 4 was correlated with both absolute and

374 normalized speed (absolute speed $R^2 = 0.460$, $p<0.05$; normalized speed $R^2 = 0.494$, $p<0.05$).

375 Likewise, the phase lag between left legs 1 and 4 was correlated with both absolute and

376 normalized speed (absolute speed $R^2 = 0.488$, $p<0.05$; normalized speed $R^2 = 0.425$, $p<0.05$).

377 The phase lag of right legs 1 and 2 was correlated with absolute speed but not normalized speed

378 (absolute speed $R^2 = 0.459$, $p<0.05$; normalized speed $R^2 = 0.336$, $p=0.109$).

379   Mean values from phase lag histograms can be used to reconstruct an average gait (Wilson,

380 1967). The stepping pattern for ipsilateral legs on the left side is shown in Fig. 5, unsurprisingly

381 the resulting sequence matches the 4 1 3 2 observed in Fig. 3 B,C suggesting that this is the

382 dominant sequence for ipsilateral legs. Likewise, the reconstructed stepping pattern for right

383 ipsilateral legs was also 4 1 3 2, with legs 4 and 2 moving almost simultaneously.

384 *Position and velocity of legs*

385 Fig. 6 shows the relationship between the angular positions and velocities of legs 1, 2, 3 and 4

386 for all sequences. This representation of leg movements in their phase plane allows the

387 examination of temporal stability of leg movement. Whilst subjects and sequences both show

388 variation mainly due to differences in speed, these plots prove useful in examining general

389 cyclic patterns of movement which allow us to infer the relative roles of each leg during

390 locomotion.

391   The phase portrait of leg 1 (Fig. 6A) again reinforces that the movement of this leg is much
392   more variable than other legs. It should be noted that this variability is not accumulated as a
393   result of combining different sequences but exists in individual sequences. Leg 2 showed
394   reasonably stable cycling which is symmetrically distributed around approximately 20 (Fig.
395   6B). Likewise, leg 3 showed reasonably stable cycling which is symmetrically distributed
396   around approximately -10 (Fig. 6C). Conversely, leg 4 varied considerably, suggesting that it
397   is possibly acting under the influence of other legs (Fig. 6D).

398   Average distance covered by the tibia is greater in legs 1 and 4 than legs 2 and 3 (Table 1).
399   Conversely, the angular distance covered in the swing phase by legs 2 and 3 is greater than legs
400   1 and 4 (Table 1). Likewise, the magnitude of the average angular velocity during the swing
401   phase is larger for legs 2 and 3 than legs 1 and 4 (Table 1). Similarly, during the stance phase
402   legs 2 and 3 experience negative velocities of greater magnitude than legs 1 and 4 (Table 1).

403   *Evaluation of the tracking algorithm*

404   Movies S1-3 included on the in the supplementary material illustrate that the algorithm appears
405   to do a reasonable job of tracking the motion of the spiders' joints across frames. Generally,
406   motion capture techniques have their accuracy assessed by comparing results to ground truth
407   data. Because we don't have access to a data set for our study species, we attempt a quantitative
408   evaluation through other techniques below.

409   Analysing 46 frames where the spider appeared stationary resulted in slightly "jiggly"
410   looking results (see Movie S3). The maximum and minimum position in x coordinates differed
411   by 2 pixels and y coordinates differed by 1 pixel. Translated in to cm x coordinate
412   measurements differed by 0.083 cm and y coordinate measurements differed by 0.042 cm.
413   Alternatively, looking at one standard deviation gave 0.557 pixels (0.023 cm) for x coordinates
414   and 0.487 pixels (0.020 cm) for y coordinates. Individual joint angles were somewhat less
415   accurate than total angle of the leg (Table 2), suggesting that at times the pose estimation fitting
416   results in one angle increasing/decreasing and a joint further down the chain does the opposite.

417   Comparing the results tracking in one direction and then the reverse direction yielded similar
418   results to above. Position data showed reasonable accuracy with root mean squared difference
419   for position in x coordinates of 2.300 pixels and y coordinates 0.983 pixels. Translated in to cm
420   x coordinate measurements differed by 0.096 cm and y coordinate measurements differed by
421   0.041 cm. Again, the angle for total leg configuration was more accurate than the angles for
422   individual joints (Table 2). Thus, results focused mainly on total leg configuration.

423

Discussion

The aim of our study was twofold: to develop a markerless technique for tracking spider locomotion and to use it to characterize the locomotion in *Dolomedes*. While markerless techniques have been an emerging area of human motion capture research for the past couple of decades, they are yet to be widely employed in the area of animal kinematics. We performed detailed analysis of locomotory behaviour in freely moving spiders without attaching physical or painted markers. Our data will now be compared with results obtained previously for spiders and other arthropods; this will be followed by an evaluation of the tracking algorithm.

Kinematic variables and speed

Both stride length and frequency were directly related to running speed, but stride frequency was more highly correlated with normalized speed and stride length was more highly correlated with absolute speed. This makes sense from a biological perspective because larger animals have longer legs, resulting in longer steps, so if other parameters remain constant this will increase absolute speed. Whereas, when speed is normalized for body length stride length has a reduced role in increasing speed and instead this is achieved by increasing stride frequency. The duration of protraction and retraction were both inversely related to stride frequency and there was no significant difference in regression slopes. This relationship is contrary to the relationship frequently observed in insects, where only retraction decreases with stride frequency and protraction remains constant (reviewed in Wilson, 1966). Results from spider species are conflicting, with some matching our observations (*Trochosa ruricola*, Ward and Humphreys, 1981) and others showing greater similarity to the trends observed in insects (*D. triton*, *Lycosa rabida* - Shultz, 1987; *L. tarantula* - Ward and Humphreys, 1981).

Inter-leg coordination

The dominant gait exhibited by *D. aquaticus* during locomotion shows similarities to several other spiders that have been studied. Like results from the tarantula (Wilson, 1967) and the jumping spider (Land, 1972), the most common stepping order of ipsilateral legs is 4 1 3 2. The functional grouping of legs is an alternating tetrapod of support, where the odd legs on the left move synchronously with the even legs on the right and vice versa in the second half of the stride. In reality, the functional groups of spiders' legs do not move in exact synchrony. The reconstructed stepping pattern from phase histograms (Fig. 5) showed legs 2 and 4 starting the stepping cycle almost simultaneously, however leg 3 lagged behind leg 1. Only a small variation in phase can result in similar stepping orders, which also resemble an alternating tetrapod gait (Wilson, 1967). The gaits of spiders *D. triton, L. rabida* (Shultz, 1987), *Hololena adnexa*, *H. curta* (Spagna et al., 2011), *Myrmarachne formicaria* (Shamble et al., 2017) and *T.*

458 *ruricola* (Ward and Humphreys, 1981) have been interpreted as an alternating. Conversely,

459 some spider species do not approach an alternating gait at even the highest speeds (Moffett and

460 Doell, 1980; Ward and Humphreys, 1981; Weihmann, 2013). It has been argued that rather

461 than a strictly alternating teterapod, spider legs should be treated as two quadrupeds in series,

462 operating slightly out-of-phase with the anterior and posterior quadrupeds less tightly coupled

463 at higher speeds (Biancardi et al., 2011).

464   Assuming *D. aquaticus* is utilizing an alternating gait, the expected phase lag values for

465 contralateral legs all to be equal to 0.5. Our results found that the coupling of legs 2-4 was

466 approximately equal to 0.5. However, the phase lag distribution for front legs was found to be

467 random. The reader can easily be convinced of this random movement by the examination of

468 the movements of legs in their phase plane (Fig. 6A). This suggests that *D. aquaticus* is actually

469 utilizing its hind three pairs of legs in an alternating tripod gait analogous to insects. The

470 alternating tripod gait predicts that contralateral and adjacent ipsilateral legs are anti-phase (i.e.

471 have phase lags of 0.5) and adjacent-but-one legs are in phase (i.e. have phase lags of 0 or 1).

472 Fig. 4 investigates some of these phase relationships, as hypothesised the phase lags of L2:L3,

473 R2:R3, L3:L4 and R3:R4 have values reasonably close to 0.5; and the phase lags of L2:L4 and

474 R2:R4 have values reasonably close to 1.

475   Phase lag relationships in the burrow dwelling wolf spider, *L. tarantula*, and the fishing

476 spider, *D. triton,* exhibit similarities to the ones described here. In *L. tarantula* ipsilateral

477 relationships including right leg 1 were random, however anti-phase contralateral coupling

478 between the front legs was maintained (Ward and Humphreys, 1981). Conversely, phase lag

479 values approached 0.5 in adjacent ipsilateral legs in *D. triton,* despite contralateral coupling of

480 the front two pairs of legs being random (Shultz, 1987). *Cupiennius salei* exhibited random

481 contralateral coupling of leg 2, with the remaining contralateral leg pairs phase relations all

482 close to 0.5 (Weihmann, 2013). Ipsilateral relationships further suggested legs may act as two

483 quadrupeds with frontal leg pairs coupled and hind leg pairs coupled and remaining

484 relationships showing or random coupling (Weihmann, 2013). Other species show

485 progressively weaker contralateral coupling in leg pairs from posterior to anterior but

486 distributions were either non-random, or was not verified statistically (*Pardosu tristis* - Moffett

487 and Doell, 1980; *L. rabida* - Shultz, 1987; *Dugesiella hentz* - Wilson, 1967).

488   The minimum requirement for static stability is three legs in a tripod on the ground at all

489 times, analogous to a stool. Thus, spiders can attain stability with a set of legs to spare, allowing

490 the function of front legs to potentially be modified for functions other than support. The range

491 of results above suggests species are adapted to use front legs for purposes other than support

492 to varying extents. Ward and Humphreys (1981) hypothesised that a possible purpose for these
493 legs is as a sensory apparatus. This was supported by observations by Blickhan and Barth
494 (1985) from tarantulas, which found that the power stroke of the front leg is shorter and the
495 vertical excursion is higher, suggesting that front legs are acting as "feelers" during locomotion.
496 Similarly, the first pair of feet of *Grammostola mollicoma* exhibit an "unusually high
497 trajectory" with longer swing phase, with the authors speculating that they probably play a
498 sensory role (Biancardi et al., 2011). These observations have been suggested as evidence that
499 front legs in spiders have been pre-adapted as an antennae-like structure and this is what allows
500 myrmecomorphic spiders to play such convincing ants, with their front legs raised and moved
501 about like antennae (Reiskind, 1977). However, recent analysis discovered that ant mimics use
502 all eight legs during locomotion which is interrupted with brief pauses where forelegs are raised
503 like ant antennae (Shamble et al., 2017). The sensory role of front legs has been hypothesised
504 in several other arthropods (stick insects - Cruse, 1976; crickets - Harris and Ghiradella, 1980;
505 whip spiders - Santer and Hebets, 2009). While waiting for prey, *D. aquaticus* use the front
506 two pairs of legs to detect vibrations both on the water and land (Forster and Forster, 1999).
507 Many species of spider are nocturnal; in the majority of these species, vision is believed to play
508 a reduced role, or no role at all, in mediating behavioural responses (Foelix, 1982). Thus, it
509 becomes particularly advantageous to use front legs as feelers when hunting at night.

510 The existence of aerial phases in terrestrial locomotion of two rapidly running spider
511 species, without any obvious gait transitions suggests large, rapidly moving, spiders likely
512 exploit dynamic rather than static stability (Spagna et al., 2011). During passive dynamic
513 walking, there is an impulsive foot-ground collision within each stride, this impact results in
514 loss of energy. The forces involved in the collision are the major determinant of locomotor
515 efficiency (Garcia et al., 2000), thus providing a significant constraint on gait generation. When
516 applied to locomotion in more complex conditions, passive dynamic simulations find it is more
517 efficient to be able to predict ground compliance and pre-emptively modify gait parameters
518 accordingly, rather than recover the trajectory after the collision (Chyou et al., 2011). This
519 implies that if spiders are indeed operating under passive dynamic principles, sensory
520 information would allow disturbances to normal locomotion to be anticipated and compensated
521 for. Therefore, front legs acting as sense organs would play a crucial role in locomotor agility.

522 Alternatively, the function of these legs has been modified due to habitat usage. Both *D.*
523 *aquaticus* and *D. triton* are semi-aquatic spiders. During locomotion on the water, a rowing
524 gait involving the legs 2 and 3 is predominately used by *D. triton*, with hind legs sometimes
525 dragged in contact with the water surface (Suter and Wildman, 1999). Lack of use of the front

526 and hind pairs of legs during terrestrial locomotion may be as a result of adaptations relating

527 to the aquatic environment. The fact that *L. tarantula* also exhibits some adaptation in front

528 legs makes this unlikely since this species more or less stays in its burrow waiting for prey to

529 pass (Ward and Humphreys, 1981). Information about terrain height and compliance can be

530 estimated using visual cues. However, this is a non-trivial computational problem requiring

531 eyes looking forward and down, plus neural circuitry capable of performing the analysis. To

532 be effective, especially in dark, highly confined spaces, a spider needs reliable sensing such as

533 that provided by antennae or tactile sensors. Even humans often revert to using poles and

534 probing when on complex unfamiliar terrain. Thus, the most likely explanation is that the front

535 pair of legs is being used as a sensory apparatus.

536 *Spider leg movements*

537 A previous study, in which walking legs were autotomized, revealed that spiders are capable

538 of adaptive changes and can replace the role of each other during locomotion (Wilson, 1967).

539 Despite this plasticity, the biomechanics of joints are important and our results suggest that

540 each leg plays a distinct role in locomotion. Analysis of the leg trajectories through phase

541 diagrams (Fig. 6) show that each leg exhibits a distinctive pattern. Legs 1 and 2 show mainly

542 positive angular position values, suggesting these legs are used to pull the body forward.

543 Conversely, legs 3 and 4 show mainly negative values so are likely used to push the body.

544 Comparisons between the amplitude of angular velocity of each leg show that legs 2 and 3

545 undergo much larger positive and negative velocities throughout the cycle. This supports the

546 hypothesis that it is predominantly legs 2 and 3 that are generating propulsive thrust, through

547 pulling and pushing respectively, throughout the locomotory cycle.

548 The conclusions drawn above are supported by additional experimental results defining leg

549 movement. Analysis of legs during the swing phase (Table 1) found that legs 2 and 3 undergo

550 larger excursions than legs 1 and 4. Additionally, excursion during the swing phase shows a

551 positive relationship with stride duration in legs 3 and 4, suggesting that in order to increase

552 speed these legs decrease the size of excursion and instead increase frequency. Reinforcing the

553 results of the phase diagrams, legs 2 and 3 produced velocities of greater magnitude than legs

554 1 and 4 in both the swing and stance phases (Table 1). For each leg there was no difference in

555 these magnitudes relative to stride period in the swing phase. However, in the stance phase legs

556 2 and 3 had negative velocities which were larger in magnitude for shorter stride periods (Table

557 1).

558 Specialization in the role of different legs is reasonably common in other arthropods. Jamon

559 and Clarac (1995) found that legs 3 and 4 were the main legs used during crayfish locomotion,

560 although in some animals these patterns were altered so legs 4 and 5 played the dominant role

561 instead. In the rapidly running cockroach, *Periplaneta americana*, different gaits utilize

562 different number of legs generating propulsion. Full and Tu (1991) found that at slow speeds

563 these cockroaches use the alternating tripod gait typical of insect walking, but in order to

564 overcome limitations in stride length, and thus increase speed, animals run primarily on their

565 two hind legs.

566 *Markerless tracking*

567 The efficiency of motion capture algorithms is generally evaluated on three criteria: the cost

568 and ease of experimental setup, the manual user intervention required and lastly the accuracy

569 of tracking results (Zakotnik and Dürr, 2005). The presented algorithm requires little in terms

570 of equipment, with the key requirements being some sort of behavioural arena which can be

571 filmed from above using a digital video camera. The resulting video sequence is analysed in

572 MATLAB using a constrained kinematic model. The model in this case was rather basic,

573 consisting of a stick spider based on experimentally determined joint lengths and constrained

574 by experimentally determined joint limits (Reußenzehn, 2008). Knowledge of joint limits is

575 not a prerequisite; it does however help constrain the state space. Currently the algorithm

576 requires that the user initializes the size and position of the spider for a given sequence and

577 specify some parameters relating to the CRF. This is done with relative ease through a graphical

578 user interface and is preferable to standard marker-based techniques which may fail in a given

579 frame due to marker occlusion or marker-like reflections etc and require manual correction and

580 re-analysis of subsequent frames. It is somewhat difficult to assess the accuracy of the

581 algorithm without ground truth data; this is attempted through both qualitative and quantitative

582 techniques. Visual inspection video sequences overlaid with the spider model verify that the

583 algorithm performs reasonably well at finding the pose of the subject. For global position,

584 results were highly repeatable with *x-y* coordinates differing by less than 1mm in each

585 dimension when data was compared running the sequence of frames in forward then reverse

586 order. Individual joint angles appeared less accurate than total leg angle (Table 2). Root mean

587 squared differences between forward and reverse tracking for total leg angle average 4.26

588 across the four legs.

589 Finally, we openly admit several limitations in the current algorithm and suggest potential

590 improvements. As mentioned previously, individual joints appear somewhat less accurate than

591 the total angle of the leg, suggesting that the optimization framework is causing one angle to

592 increase/decrease and a joint further down the limb to do the opposite. An attempt was made

593 to avoid this by having angular rotations occur from segments closest to the body outwards,

594 but because the angles and corresponding energy term are recalculated several times per frame
595 this was not as successful as anticipated. If improvements are made to the speed of the
596 algorithm, it becomes feasible to run each sequence a number of times and then calculate pose
597 based on the distribution of results rather than a single run. Similarly, repeated analysis could
598 be done on each frame and a disambiguation method could be used to select one of the poses
599 as the correct solution. Such a technique has been implemented for marker-based motion
600 capture which uses stochastic optimization, rather than relying solely on segmentation, to
601 determine the position of markers (Zakotnik and Dürr, 2005). The disambiguation method
602 described in this research is based on the Viterbi method for Markov chains and works by
603 processing the entire sequence, then selecting the trajectory which is globally smoothest for all
604 joint angles and frames (Zakotnik and Dürr, 2005).

605 Knowledge about the mechanical properties of spider limbs and the physics involved in
606 locomotion helps constrain the state space required for movement. The more we know about
607 the spiders' mechanical design, the easier the task of tracking becomes. The current tracking
608 algorithm only makes use of the very basic assumption of constant velocity to predict the pose
609 of the spider in the next frame. If we had an accurate physical model of the spider our
610 predictions would be improved, which in turn makes the statistical modelling easier. Research
611 is ongoing relating joint angles to applied torque, investigating the use of haemolymph to
612 hydraulically extend the legs and creating simulated passive dynamic walkers.

613 With monocular techniques, many possible poses can explain the same spider shape
614 observed in the image. Multiple views can be used to reduce the ambiguity in pose. To maintain
615 the simplicity of a single camera setup, the view from the top and side can be simultaneously
616 recorded by arranging a mirror set at 45 from the animal plane. Using the PoseCut approach
617 multiple views can be easily incorporated into a single optimization framework (Bray et al.,
618 2006).

619 *Conclusions*

620 The markerless tracking algorithm proved successful in tracking spiders during locomotion.
621 This represents a step away from the traditional marker-based techniques towards computer
622 vision-based approaches, which helps avoid some of the difficulties of marking small animals.

623 Stride frequency showed a greater correlation with normalized speed than absolute speed
624 and stride length showed a greater correlation with absolute speed than normalized speed. This
625 suggests that larger animals increase their speed by increasing stride length, whereas it is
626 possible for smaller animals to increase their speed by increasing stride frequency. Contrary to

627 the relationship frequently observed in insects and some spiders, both protraction and retraction
628 periods decreased with speed.

629 Each leg was found to contribute in a specific manner to locomotion. Movements of front
630 legs were random suggesting they play some other role, possibly sensory, rather than
631 contributing to stability. The 2nd and 3rd pairs appeared to play a more dominant role in
632 generating propulsive force, with hind legs probably contributing more to stability than
633 propulsion.

634 Now that there is a basic understanding of the biomechanics behind terrestrial locomotion,
635 it is possible to begin exploring how locomotion varies under different conditions and how the
636 nervous system produces these changes.

637

List of abbreviations

A Anterior

AEP Anterior extreme position

CRF Conditional random field

GUI Graphical user interface

L Left

P Posterior

PEP Posterior extreme position

R Right

Competing interests

No competing interests declared.

Author contributions

Conceptualization: K.F.P., M.G.P.; Methodology: K.F.P., M.G.P.; Software: K.F.P.; Validation: K.F.P.; Formal analysis: K.F.P.; Investigation: K.F.P.; Resources: K.F.P., M.G.P.; Data curation: K.F.P.; Writing - original draft: K.F.P..; Writing - review & editing K.F.P., M.G.P.; Visualization: K.F.P.; Supervision: M.G.P.; Project administration: K.F.P., M.G.P., Funding acquisition: M.G.P.

References

Amaya, C. C., Klawinski, P. D. and Formanowicz, J., Daniel R. (2001). The effects of leg autotomy on running speed and foraging ability in two species of wolf spider, (Lycosidae). *Am. Midl. Nat.* **145**, 201–205.

Anderson, J. F. and Prestwich, K. N. (1975). The fluid pressure pumps of spiders (Chelicerata, Araneae). *Z. Für Morphol. Tiere* **81**, 257–277.

Apontes, P. and Brown, C. A. (2005). Between-sex variation in running speed and a potential cost of leg autotomy in the wolf spider *Pirata sedentarius*. *Am. Midl. Nat.* **154**, 115–125.

Bender, J. A., Simpson, E. M. and Ritzmann, R. E. (2010). Computer-assisted 3D kinematic analysis of all leg joints in walking insects. *PLoS ONE* **5**, e13617.

Berman, G. J., Choi, D. M., Bialek, W. and Shaevitz, J. W. (2014). Mapping the stereotyped behaviour of freely moving fruit flies. *J. R. Soc. Interface* **11**, 20140672.

Biancardi, C. M., Fabrica, C. G., Polero, P., Loss, J. F. and Minetti, A. E. (2011). Biomechanics of octopedal locomotion: kinematic and kinetic analysis of the spider *Grammostola mollicoma*. *J. Exp. Biol.* **214**, 3433–3442.

Blickhan, R. (1986). Stiffness of an arthropod leg joint. *J. Biomech.* **19**, 375–384.

Blickhan, R. and Barth, F. G. (1985). Strains in the exoskeleton of spiders. *J. Comp. Physiol. A* **157**, 115–147.

Booster, N. A., Su, F. Y., Adolph, S. C. and Ahn, A. N. (2015). Effect of temperature on leg kinematics in sprinting tarantulas (*Aphonopelma hentzi*): high speed may limit hydraulic joint actuation. *J. Exp. Biol.* **218**, 977–982.

Bowerman, R. F. (1975a). The control of walking in the scorpion. I. Leg movements during normal walking. *J. Comp. Physiol.* **100**, 183–196.

Bowerman, R. F. (1975b). The control of walking in the scorpion. II. Coordination modification as a consequence of appendage ablation. *J. Comp. Physiol.* **100**, 197–209.

Bowerman, R. F. (1976). An electrophysiological survey of joint receptors in the walking legs of the scorpion, *Paruroctonus mesaensis*. *J. Comp. Physiol.* **105**, 353–366.

Bowerman, R. F. (1977). The control of arthropod walking. *Comp. Biochem. Physiol. A Physiol.* **56**, 231–247.

Bowerman, R. F. and Burrows, M. (1980). The morphology and physiology of some walking leg motor neurones in a scorpion. *J. Comp. Physiol.* **140**, 31–42.

Boykov, Y. and Kolmogorov, V. (2004). An experimental comparison of min-cut/max- flow algorithms for energy minimization in vision. *IEEE Trans. Pattern Anal. Mach. Intell.* **26**, 1124–1137.

703 **Bray, M., Kohli, P. and Torr, P. H. S.** (2006). PoseCut: Simultaneous segmentation and 3D
704   pose estimation of humans using dynamic graph-cuts. In *Computer Vision – ECCV*
705   *2006*, pp. 642–655. Springer, Berlin, Heidelberg.

706 **Bregler, C., Malik, J. and Pullen, K.** (2004). Twist based acquisition and tracking of animal
707   and human kinematics. *Int. J. Comput. Vis.* **56**, 179–194.

708 **Brown, A. E. X. and Bivort, B. de** (2018). Ethology as a physical science. *Nat. Phys.* 1.

709 **Chyou, T., Liddell, G. F. and Paulin, M. G.** (2011). An upper-body can improve the
710   stability and efficiency of passive dynamic walking. *J. Theor. Biol.* **285**, 126–135.

711 **Cruse, H.** (1976). The function of the legs in the free walking stick insect, *Carausius*
712   *morosus*. *J. Comp. Physiol.* **112**, 235–262.

713 **Dickinson, M. H., Farley, C. T., Full, R. J., Koehl, M. a. R., Kram, R. and Lehman, S.**
714   (2000). How Animals Move: An Integrative View. *Science* **288**, 100–106.

715 **Dillon, L. S.** (1952). The myology of the araneid leg. *J. Morphol.* **90**, 467–480.

716 **Ellis, C. H.** (1944). The mechanism of extension in the legs of spiders. *Biol. Bull.* **86**, 41–50.

717 **Favreau, L., Reveret, L., Depraz, C. and Cani, M. P.** (2006). Animal gaits from video:
718   Comparative studies. *Graph. Models* **68**, 212–234.

719 **Fisher, N. I.** (1995). *Statistical analysis of circular data*. Cambridge: Cambridge University
720   Press.

721 **Foelix, R. F.** (1982). *Biology of spiders*. Cambridge, MA: Harvard University Press.

722 **Fontaine, E. I., Zabala, F., Dickinson, M. H. and Burdick, J. W.** (2009). Wing and body
723   motion during flight initiation in Drosophila revealed by automated visual tracking. *J.*
724   *Exp. Biol.* **212**, 1307–1323.

725 **Forster, R. and Forster, L.** (1999). *Spiders of New Zealand and their worldwide kin.*
726   Dunedin: University of Otago Press.

727 **Fourtner, C. R. and Sherman, R. G.** (1973). Chelicerate skeletal neuromuscular systems.
728   *Integr. Comp. Biol.* **13**, 271–289.

729 **Full, R. J. and Tu, M. S.** (1991). Mechanics of a rapid running insect: two-, four- and six-
730   legged locomotion. *J. Exp. Biol.* **156**, 215–231.

731 **Gall, J., Stoll, C., Aguiar, E. de, Theobalt, C., Rosenhahn, B. and Seidel, H. P.** (2009).
732   Motion capture using joint skeleton tracking and surface estimation. In *2009 IEEE*
733   *Conference on Computer Vision and Pattern Recognition*, pp. 1746–1753.

734 **Gambaretto, E. and Corazza, S.** (2009). Markerless motion capture: the challenge of
735   accuracy in capturing animal motions through model based approaches. p. 74470E.
736   International Society for Optics and Photonics.

737 **Garcia, M., Chatterjee, A. and Ruina, A.** (2000). Efficiency, speed, and scaling of two-
738   dimensional passive-dynamic walking. *Dyn. Stab. Syst.* **15**, 75–99.

739 **Gerald, G. W., Thompson, M. M., Levine, T. D. and Wrinn, K. M.** (2017). Interactive
740   effects of leg autotomy and incline on locomotor performance and kinematics of the
741   cellar spider, *Pholcus manueli. Ecol. Evol.* **7**, 6729–6735.

742 **Gibson, D. P., Campbell, N. W. and Thomas, B. T.** (2003). Quadruped gait analysis using
743   sparse motion information. In *Proceedings 2003 International Conference on Image
744   Processing*, pp. 333–336.

745 **Gowda, S. B. M., Paranjpe, P. D., Reddy, O. V., Thiagarajan, D., Palliyil, S., Reichert,
746   H. and VijayRaghavan, K.** (2018). GABAergic inhibition of leg motoneurons is
747   required for normal walking behavior in freely moving Drosophila. *Proc. Natl. Acad.
748   Sci.* **115**, E2115–E2124.

749 **Greig, D. M., Porteous, B. T. and Seheult, A. H.** (1989). Exact maximum a posteriori
750   estimation for binary images. *J. R. Stat. Soc. Ser. B Methodol.* **51**, 271–279.

751 **Harris, J. and Ghiradella, H.** (1980). The forces exerted on the substrate by walking and
752   stationary crickets. *J. Exp. Biol.* **85**, 263–279.

753 **Hughes, G. M.** (1952). The co-ordination of insect movements: I The walking movements of
754   insects. *J. Exp. Biol.* **29**, 267–285.

755 **Jamon, M. and Clarac, F.** (1995). Locomotor patterns in freely moving crayfish
756   (*Procambarus clarkii*). *J. Exp. Biol.* **198**, 683–700.

757 **Jensen, R. R., Paulsen, R. R. and Larsen, R.** (2009). Analyzing gait using a time-of-flight
758   camera. In *Image Analysis. SCIA 2009, Lecture Notes in Computer Science*, pp. 21–
759   30. Springer, Berlin, Heidelberg.

760 **Klibaite, U., Berman, G. J., Cande, J., Stern, D. L. and Shaevitz, J. W.** (2017). An
761   unsupervised method for quantifying the behavior of paired animals. *Phys. Biol.* **14**,
762   015006.

763 **Land, M. F.** (1972). Stepping movements made by jumping spiders during turns mediated by
764   the lateral eyes. *J. Exp. Biol.* **57**, 15–40.

765 **Maier, L., Root, T. M. and Seyfarth, E.-A.** (1987). Heterogeneity of spider leg muscle:
766   Histochemistry and electrophysiology of identified fibers in the claw levator. *J.
767   Comp. Physiol. B* **157**, 285–294.

768 **Moeslund, T. B., Hilton, A. and Krüger, V.** (2006). A survey of advances in vision-based
769   human motion capture and analysis. *Comput. Vis. Image Underst.* **104**, 90–126.

770 **Moffett, S. and Doell, G. S.** (1980). Alteration of locomotor behavior in wolf spiders
771   carrying normal and weighted egg cocoons. *J. Exp. Zool.* **213**, 219–226.

772 **Parry, D. A.** (1957). Spider leg-muscles and the autotomy mechanism. *J. Cell Sci.* **s3-98**,
773   331–340.

774 **Parry, D. A. and Brown, R. H. J.** (1959a). The hydraulic mechanism of the spider leg. *J.*
775   *Exp. Biol.* **36**, 423–433.

776 **Parry, D. A. and Brown, R. H. J.** (1959b). The jumping mechanism of salticid spiders. *J.*
777   *Exp. Biol.* **36**, 654–664.

778 **Reiskind, J.** (1977). Ant-mimicry in Panamanian clubionid and salticid spiders (Araneae:
779   Clubionidae, Salticidae). *Biotropica* **9**, 1–8.

780 **Reußenzehn, S.** (2008). Analysis of ranges of movement for leg joints of the hunting spider
781   Dolomedes aquaticus. PGDipSci Dissertation, University of Otago, Dunedin.

782 **Reußenzehn, S.** (2010). Mechanical design of the legs of Dolomedes aquaticus - Novel
783   approaches to quantify the hydraulic contribution to joint movement and to create a
784   segmented 3D spider model. MSc thesis, University of Otago, Dunedin.

785 **Santer, R. D. and Hebets, E. A.** (2009). Tactile learning by a whip spider, *Phrynus*
786   *marginemaculatus* C.L. Koch (Arachnida, Amblypygi). *J. Comp. Physiol. A* **195**,
787   393–399.

788 **Sensenig, A. T. and Shultz, J. W.** (2006). Mechanical energy oscillations during locomotion
789   in the harvestman *Leiobunum vittatum* (Opiliones). *J. Arachnol.* **34**, 627–633.

790 **Shamble, P. S., Hoy, R. R., Cohen, I. and Beatus, T.** (2017). Walking like an ant: a
791   quantitative and experimental approach to understanding locomotor mimicry in the
792   jumping spider *Myrmarachne formicaria*. *Proc R Soc B* **284**, 20170308.

793 **Shultz, J. W.** (1987). Walking and surface film locomotion in terrestrial and semi-aquatic
794   spiders. *J. Exp. Biol.* **128**, 427–444.

795 **Shultz, J. W.** (1991). Evolution of locomotion in arachnida: The hydraulic pressure pump of
796   the giant whipscorpion, *Mastigoproctus giganteus* (Uropygi). *J. Morphol.* **210**, 13–31.

797 **Siebert, T., Weihmann, T., Rode, C. and Blickhan, R.** (2010). *Cupiennius salei*:
798   biomechanical properties of the tibia–metatarsus joint and its flexing muscles. *J.*
799   *Comp. Physiol. B* **180**, 199–209.

800 **Spagna, J. C., Goldman, D. I., Lin, P. C., Koditschek, D. E. and Full, R. J.** (2007).
801   Distributed mechanical feedback in arthropods and robots simplifies control of rapid
802   running on challenging terrain. *Bioinspir. Biomim.* **2**, 9–18.

803 **Spagna, J. C., Valdivia, E. A. and Mohan, V.** (2011). Gait characteristics of two fast-
804   running spider species (*Hololena adnexa* and *Hololena curta*), including an aerial
805   phase (Araneae: Agelenidae). *J. Arachnol.* **39**, 84–91.

806 **Suter, R. B. and Wildman, H.** (1999). Locomotion on the water surface: hydrodynamic
807   constraints on rowing velocity require a gait change. *J. Exp. Biol.* **202**, 2771–2785.

808 **Uhlmann, V., Ramdya, P., Delgado-Gonzalo, R., Benton, R. and Unser, M.** (2017).
809   FlyLimbTracker: An active contour based approach for leg segment tracking in
810   unmarked, freely behaving *Drosophila*. *PLOS ONE* **12**, e0173433.

811   **Ward, T. M. and Humphreys, W. F.** (1981). Locomotion in burrowing and vagrant wolf
812   spiders (Lycosidae). *J. Exp. Biol.* **92**, 305–321.

813   **Weihmann, T.** (2013). Crawling at high speeds: steady level locomotion in the spider
814   *Cupiennius salei* - global kinematics and implications for centre of mass dynamics.
815   *PLOS ONE* **8**, e65788.

816   **Wilson, D. M.** (1966). Insect walking. *Annu. Rev. Entomol.* **11**, 103–122.

817   **Wilson, D. M.** (1967). Stepping patterns in tarantula spiders. *J. Exp. Biol.* **47**, 133–151.

818   **Wilson, R. S.** (1970). Some comments on the hydrostatic system of spiders (Chelicerata,
819   Araneae). *Z. Für Morphol. Tiere* **68**, 308–322.

820   **Wilson, R. S. and Bullock, J.** (1973). The hydraulic interaction between prosoma and
821   opisthosoma in *Amaurobius ferox* (Chelicerata, Araneae). *Z. Für Morphol. Tiere* **74**,
822   221–230.

823   **Winter, D. A.** (1990). *Biomechanics and motor control of human movement*. New York:
824   John Wiley & Sons.

825   **Zakotnik, J. and Dürr, V.** (2005). Motion analysis using stochastic optimisation and posture
826   disambiguation. In *Proceedings of the 3rd International Symposium on Adaptive
827   Motion in Animals and Machines (AMAM2005, Ilmenau, Germany, September 25th -
828   30th).*

829   **Zar, J. H.** (1996). *Biostatistical analysis*. 3rd ed. Upper Saddle River, N.J.: Prentice Hall.

830   **Zeng, Y. and Crews, S.** (2018). Biomechanics of omnidirectional strikes in flat spiders. *J.
831   Exp. Biol.* **221**, jeb166512.

832

Figures

A

B

C
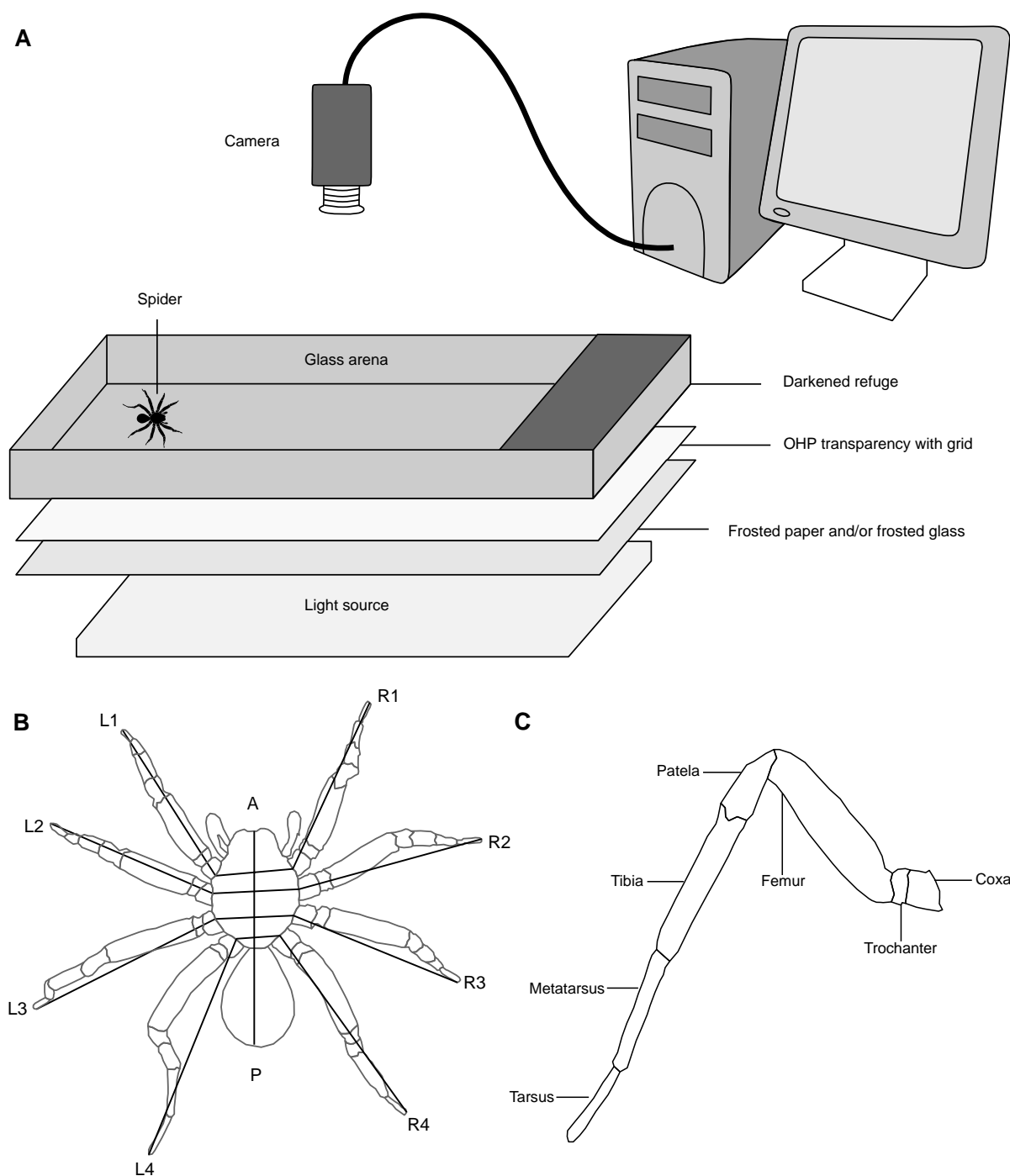
Fig. 1. Experimental setup and study animal. (A) Experimental setup consists of a glass arena with a darkened refuge at one end. The arena is lit by LED arrays scattered using frosted paper and/or frosted glass. A video camera films the spider from above. The camera was attached to a computer, which was used for image capture, storage and analysis. For further details see text. (B) Locomotor appendages of the spider. Leg movements were based on the angle delimited by the tarsus, the body-Coxa joint of a given leg and the body-Coxa joint of the contralateral leg. This angle was equal to 0 when the leg was perpendicular to the cephalo-caudal axis of the body. Its value increased when the leg moved forwards towards the AEP and decreased when the leg moved backwards towards the PEP. (C) Morphology of the spider leg showing the segments involved in locomotion.
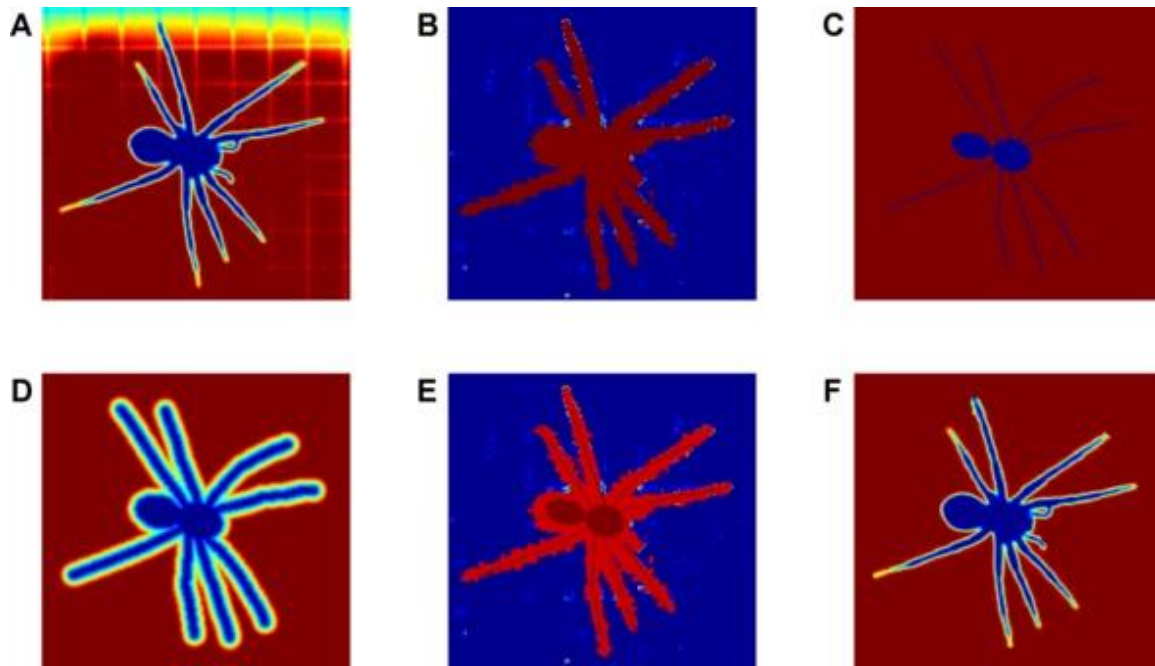
844

Fig. 2. Different terms in our image segmentation and pose estimation algorithm. (A) Original image. (B) Likelihood of pixels being labelled background. (C) The stick spider model after optimization of its 2D pose. (D) The shape prior (distance transform) corresponding to the optimal pose of the stick spider. (E) Likelihood of pixels being labelled background after incorporation of the shape prior. (F) The segmentation result obtained by the algorithm which is the maximum a posteriori solution of the energy of the pose specific CRF.
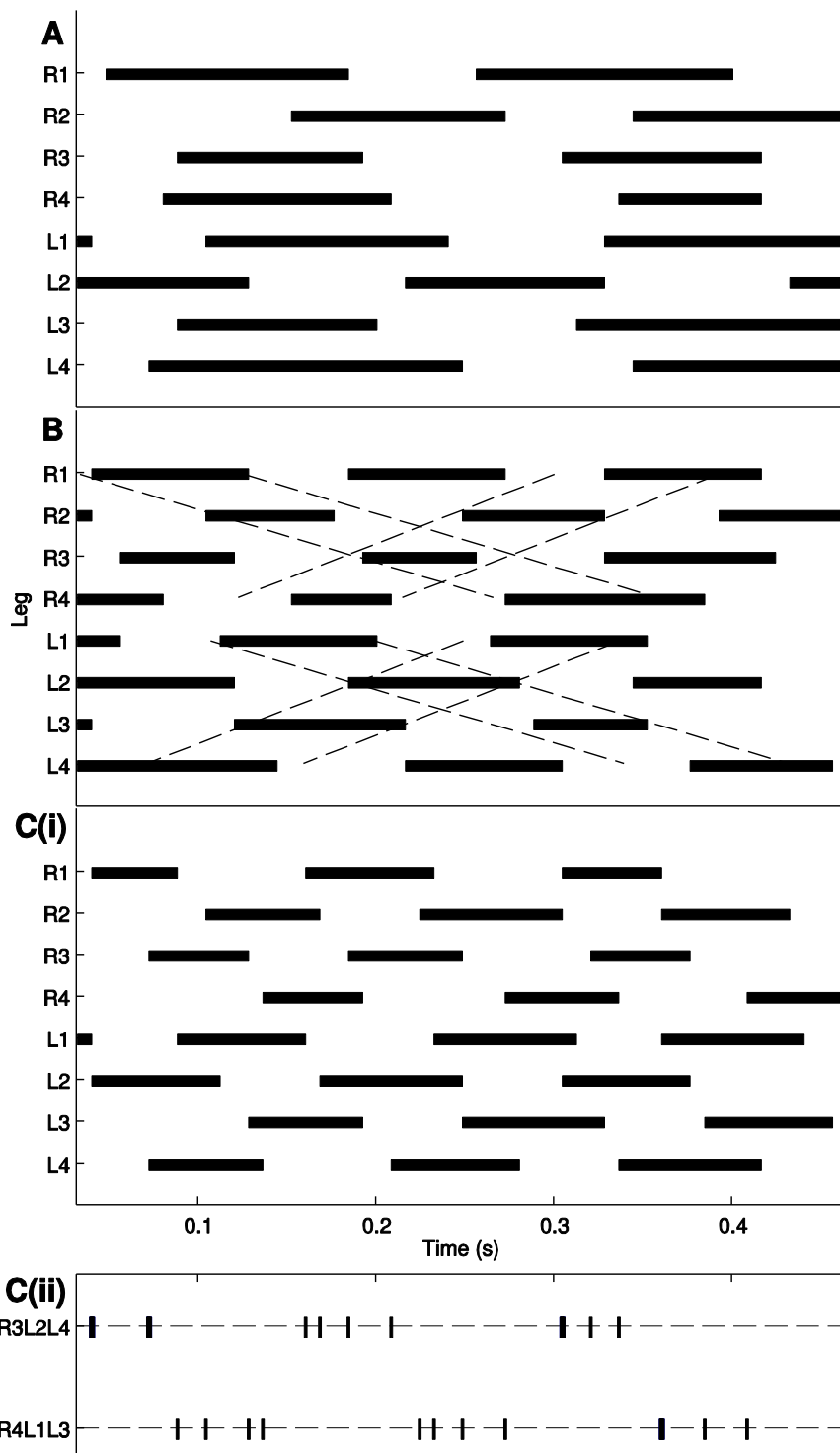
850

851

Fig. 3. Stepping pattern diagrams from a single spider at a range of speeds. The heavy black lines represent stance phase (retraction) and the spaces swing phase (protraction). (A) Average speed 15.963 cm s^{-1}, stride frequency 5.142 Hz and stride length 3.116 cm. (B) Average speed 24.286 cm s^{-1}, stride frequency 6.632 Hz and stride length 3.691 cm. Dashed lines illustrate apparent forward or backward metachronal waves. (C) Average speed 33.306 cm s^{-1}, stride frequency 8.403 Hz and stride length 3.997 cm. (C (ii)) The data is rearranged to emphasise functional leg groups. Onset of retraction is represented by a vertical line; the alternating tetrapod is more evident. The scale is located at the bottom of C (i).
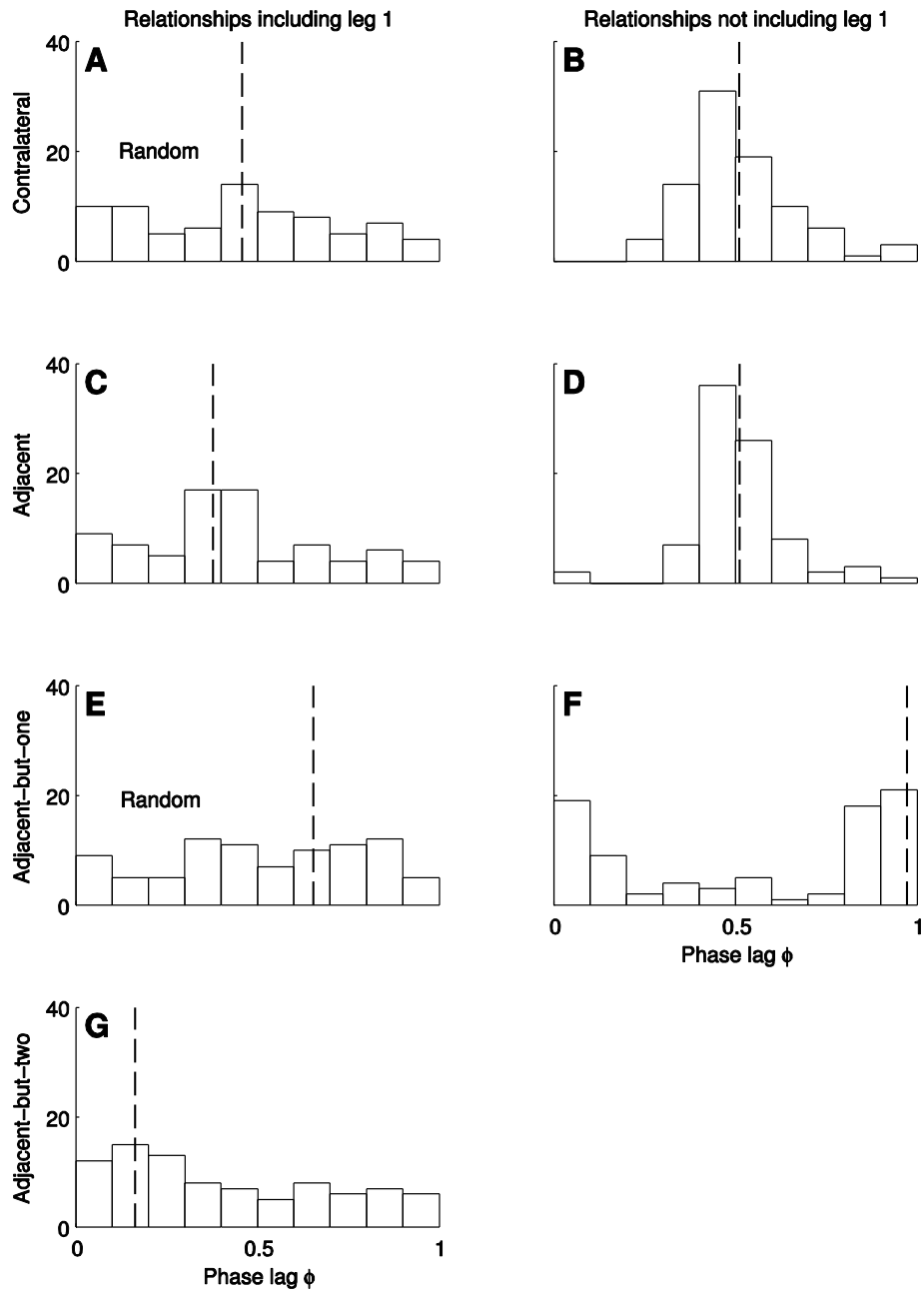
859

860

Fig. 4. Phase histograms showing the time at which an AEP occurred for a given leg relative within the period of the reference leg. Representative plots were chosen to illustrate different couplings and relationships. (A) Contralateral legs R1:L1. (B) Contralateral legs R4:L4. (C) Adjacent ipsilateral legs R1:R2. (D) Adjacent ipsilateral legs R3:R4. (E) Adjacent-but-one ipsilateral legs R1:R3. (F) Adjacent-but-one ipsilateral legs R2:R4. (G) Adjacent-but-two ipsilateral legs R1:R4. Trends illustrated in C-G were similar for legs on the left-hand side. Dashed lines represent the circular mean. The phase lag distribution for (A) L1:R1 and (E) R1:R3 is random.
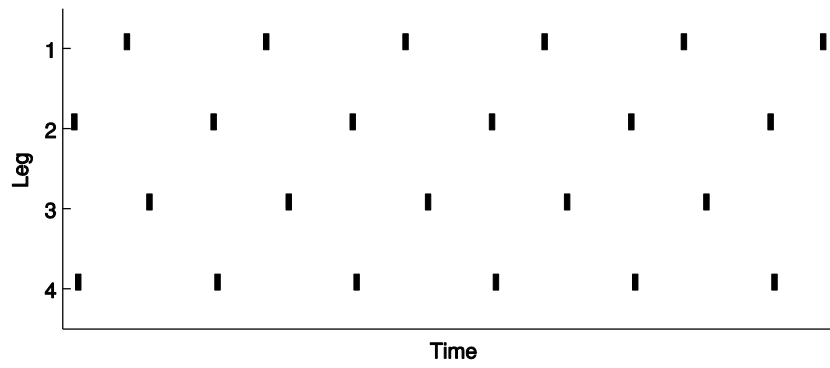
867

868

Fig. 5. Stepping pattern reconstruction of ipsilateral legs from peak values from the phase histograms. The
vertical lines represent the start of each stepping cycle. Reconstructed average gait 4132. Phases used in this case
were the left legs; however, using right legs did not alter the reconstructed average gait.
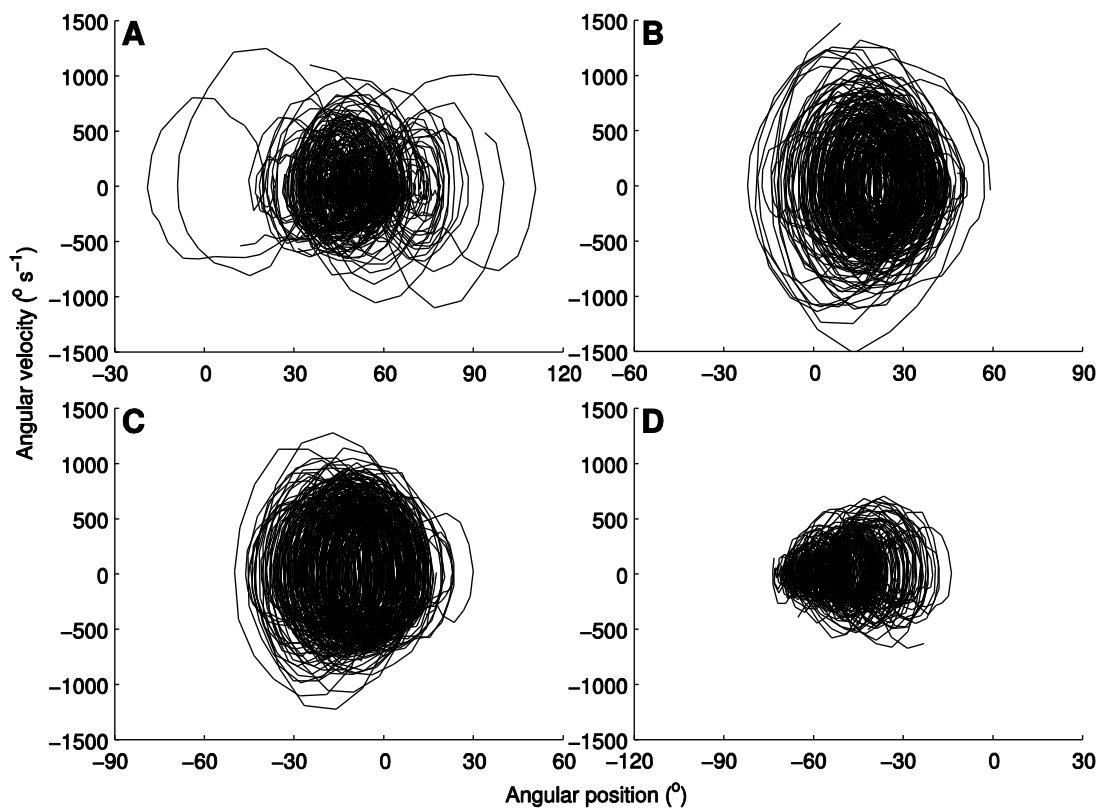
872

873

Fig. 6. Movements of the legs in their phase plane. Angular speeds plotted as a function of angular positions.
Strides occurring during all sequences have been superimposed (N=27). (A) leg 1. (B) leg 2. (C) leg 3. (D) leg 4.
Angular position is equal to zero when the leg is perpendicular to the body axis of symmetry, while the x-values
differ in magnitude each graph has the same size scale and displays the same range.

878

Tables

Table 1. Mean values for distance travelled by the tarsus during swing phase (cm), angular excursion ($^\circ$), average angular velocity ($^\circ$ s^{-1}) in both swing and stance phases for each leg pair.

Leg	*Mean $\pm$ S.D.*	*Group Differences*
Distance travelled by tarsus		
1	1.376 $\pm$ 0.305	>2, 3
2	0.817 $\pm$ 0.176	<1, 4, >3
3	0.576 $\pm$ 0.174	<1, 2, 4
4	1.299 $\pm$ 0.299	> 2, 3
$F_{3,112}$= 70.503, p<0.001		
Angular excursion		
1	13.734 $\pm$ 4.183	<2, 3, >4
2	22.029 $\pm$ 5.596	>1, 4
3	24.273 $\pm$ 4.329	>1, 4
4	10.102 $\pm$ 4.051	<1, 2, 3
$F_{3,112}$= 62.305, p<0.001		
Swing velocity		
1	196.965 $\pm$ 50.949	<2, 3
2	321.688 $\pm$ 92.472	>1, 4
3	357.535 $\pm$ 51.099	>1, 4
4	158.431 $\pm$ 59.718	<2, 3
$F_{3,112}$= 61.604, p<0.001		
Stance velocity		
1	-189.046 $\pm$ 58.274	<4, >2, 3
2	-299.612 $\pm$ 87.688	<1, 4
3	-328.007 $\pm$ 57.650	<1, 4
4	-135.792 $\pm$ 40.551	>1, 2, 3
$F_{3,112}$= 59.592, p<0.001		

F and p values are from one-way ANOVA.
Group differences were determined by post-hoc Tukey's test.

882
883 **Table 2.** Verification of tracking accuracy via two approaches: 1) differences between maximum and minimum
884 values ($^\circ$) over a sequence of frames where the spider was reasonably stationary; 2) root mean squared
885 differences ($^\circ$) between forward and reverse tracking for a single sequence.

| | Range ($^\circ$) for stationary frames | | | | Root mean squared differences ($^\circ$) | | | |
| | Leg | | | | Leg | | | |
Joint	1	2	3	4	1	2	3	4
Body-Co	5 (1.502)	13 (3.468)	6 (1.814)	5 (1.268)	4.739	5.395	5.185	5.827
Co-Tr	9 (2.581)	14 (3.865)	8 (2.465)	2 (0.643)	6.760	5.604	7.050	5.594
Pa-Ti	5 (1.730)	14 (3.793)	3 (0.643)	7 (2.248)	6.417	3.969	4.636	3.988
Ti-Me	9 (3.279)	13 (2.899)	3 (0.856)	3 (1.167)	2.006	1.882	1.408	1.225
Me-Ta	10 (3.528)	9 (2.771)	13 (5.019)	6 (2.464)	15.851	14.035	7.689	7.521
Total leg	3 (0.707)	3 (0.909)	2 (0.662)	3 (0.872)	6.166	4.311	3.311	3.252

Values were averaged over leg pairs.

886
887

888 **Supplementary material**

889 Movie S1. The markerless technique accurately segments the video stream into spider and

890 background. Filming was conducted at 125 fps but all videos in the supplementary material

891 have a play rate of 30 fps.

892

893 Movie S2. The original video overlaid with the stick spider in its estimated pose.

894

895 Movie S3. Tracking of the spider in reasonably stationary frames provides an estimate of

896 accuracy.

897